Numerical Partial Differential Equation
Peking University
Fall 2020
Yongli Peng

Homework 10

1 Problem setting

In this project we aim to solve the hyperbolic equations using 6 finite difference schemes: explicit upwind scheme, Lax-Friedrichs scheme (LF), Lax-Wendorff scheme (LW), Beam-Warming scheme (BW), Crank-Nicolson scheme (CN) and generalized MUSCL scheme. The 4 problems are:
Example 2.1: Consider the intial value problem of 1D advection equation $u_t + au_x = 0, x \in \Omega \subset \mathbb{R}, t > 0$ with a constant and intial data

$$u_0(x) = \begin{cases} 1, & x < 0, \\ 0, & x > 0, \end{cases}$$

and take $a = 1$ with the step size ratio $\tau/h = 0.5$.
Propagation of a wave packet: Consider the same 1D advection equation with $a = 1$ and the initial data consisting of a sine wave modulated by a Gaussian centered at $x = 0.5$: $u(x,0) = e^{-100(x-0.5)^2}\sin(kx)$, with k chosen so that there are 16 grid points per wavelength: $kh = 2\pi/16 \approx 0.4$. As the problem suggested, we assume $\Omega = [0,1]$, the spatial step size $h = 1/200$, the time step size $\tau = 0.8h$ and $k = 80$. Test the result at the time $t = 2, 4, 8$.
Highly discontious data: Consider the same 1D advection equation with $a = 1$ and highly discontious initial data

$$u(x,0) = \begin{cases} -\xi\sin\left(1.5\pi\xi^2\right), & \text{if } -1 \le \xi < -1/3 \\ |\sin(2\pi\xi)|, & \text{if } |\xi| < 1/3 \\ 2\xi - 1 - \sin(3\pi\xi)/6, & \text{if } 1/3 < \xi \le 1 \end{cases}$$

which is periodic in x with period 2, where $\xi = x - 0.3$ if $-0.7 \le x \le 1$ and $\xi = x + 1.7$ if $-1 \le x \le -0.7$. So we can focus on the case when $\Omega = [-1,1]$ for its periodicity.
Burger's equation: This equation can written explicitly as below:

$$\begin{cases} u_t + (u^2/2)_x = 0, x \in [0, 2\pi), t > 0 \\ u(x,0) = \sin(x), x \in [0, 2\pi) \end{cases}$$

2 Numerical schemes

We use 6 types of schemes to solve the above problems. We list them below (first for the case when a is a constant).

The explicit upwind scheme (in the case here $a > 0$):

$$\frac{u_j^{n+1} - u_j^n}{\tau} + a\frac{u_j^n - u_{j-1}^n}{h} = 0$$

The LF scheme:

$$\frac{u_j^{n+1} - \left(u_{j+1}^n + u_{j-1}^n\right)/2}{\tau} + a\frac{u_{j+1}^n - u_{j-1}^n}{2h} = 0$$

The LW scheme:

$$\frac{u_j^{n+1} - u_j^n}{\tau} + a\frac{u_{j+1}^n - u_{j-1}^n}{2h} - \tau a^2\frac{u_{j+1}^n - 2u_j^n + u_{j-1}^n}{2h^2} = 0$$

The BW scheme:

$$\frac{u_j^{n+1} - u_j^n}{\tau} + a\frac{3u_j^n - 4u_{j-1}^n + u_{j-2}^n}{2h} - \tau a^2\frac{u_j^n - 2u_{j-1}^n + u_{j-2}^n}{2h^2} = 0$$

The CN scheme:

$$\frac{u_j^{n+1} - u_j^n}{\tau} + a\frac{u_{j+1}^n - u_{j-1}^n}{4h} + a\frac{u_{j+1}^{n+1} - u_{j-1}^{n+1}}{4h} = 0$$

The generalized MUSCL scheme:

$$u_j^{n+1} = u_j^n - \lambda\left(\hat{f}(u_j^n + \frac{h}{2}S_j^n, u_{j+1}^n - \frac{h}{2}S_{j+1}^n) - \hat{f}(u_{j-1}^n + \frac{h}{2}S_{j-1}^n, u_j^n - \frac{h}{2}S_j^n)\right),$$

where $\lambda = \tau/h$ the mesh ratio, $\hat{f}$ is the numerical flux satisfying the consistent condition $\hat{f}(u,u) = f(u)$ and f is from the conservative hyperbolic PDE $u_t + (f(u))_x = 0$. In the first three problem $f(u) = au$ with $a = 1$ and in the last problem $f(u) = \frac{u^2}{2}$. And we use the numerical flux in the upwind method in this case:

$$\hat{f}(U_j^m, U_j^{m+1}) = \begin{cases} f(U_j^m), & \text{if } a_{j+1/2}^m \geq 0, \\ f(U_j^{m+1}), & \text{if } a_{j+1/2}^m < 0, \end{cases}$$

and $a_{j+1/2}^m = \frac{f(U_{j+1}^m) - f(U_j^m)}{U_{j+1}^m - U_j^m}$. So when $f = au$ with $a > 0$ we have $\hat{f}(U_j^m, U_j^{m+1}) = f(U_j^m) = aU_j^m$. Moreover we have $S_j := \operatorname{minmod}\left(\left(u_{j+1} - u_j\right)/h, \left(u_j - u_{j-1}\right)/h\right)$ with

$$\operatorname{minmod}(a,b) = \begin{cases} a, & ab > 0, |a| \leq |b| \\ b, & ab > 0, |b| \leq |a| \\ 0, & ab \leq 0 \end{cases}$$

We use the simplest, uniform mesh: $x_0 = a < x_1 < \cdots < x_N = b$ with $a = 0, b = 1$ except for the 3rd problem and in that case $a = -1, b = 1$. And we assume $x_i - x_{i-1} = \frac{b-a}{N}$. The spatial and temporal step size is set as the problem suggested. Then we can compute numerically the approximated value at these points at some discrete time point of the solution to the PDE.

Then we only need to discuss how to cope with the boundary condition for the linear problems. Note except for the first problem we can pose periodic boundary conditions on the problem. The initial function in the 3rd problem is exactly periodic, whereas in the 2nd problem though the function is not periodic, its magnitude at $0, 1$ is approximately 0 ($|u(0, 0)|, |u(1, 0)| \le e^{-25} \approx 0$). As for the first problem even if we cannot pose periodic BC, we can impose inflow BC, i.e. we assume additionally $u(0, t) = 1$. This can be easily verified when $a = 1 > 0$ and $u(x, 0) = 1$ for $x < 0$. In this way the problem is well-posed with the region $\Omega = [0, 1]$ for the 1st and 2nd problem, $\Omega = [-1, 1]$ for the 3rd problem.

As for the numerical methods, when we have periodic BC we can just use $u_1, u_2, \cdots$ to replace $u_{N+1}, u_{N+2}, \cdots$ appeared in the scheme. This generates the corresponding equation at the boundary. But if we only have inflow BC, we can first have $u_0 = 1$ at grid node 0. This will be okay for upwind method. But for LF, LW and CN method where we have the node $j + 1$ at the jth stencil we need to tackle the outflow boundary point. Here we just naively add an upwind update at this node: $u_N^{n+1} = u_N^n - \frac{a\tau}{h}(u_N^n - u_{N-1}^n)$. As for MUSCL and BW method we also have the node $j - 2$ in the jth point. So we will assume $u_0 = u_{-1} = 1$ when update u_1 (which also follows from the transportation property of the Advection PDE).

Finally we would like to generalize the above 6 methods to the case of quasi-linear equations: $u_t + (f(u))_x = 0$ and solve the Burgers equation when $f(u) = \frac{u^2}{2}$. Note here $\Omega = [0, 2\pi]$ is not easy to generate mesh. So we make a change of variable $\hat{x} = 2\pi x$ and the problem is transformed with $f(u) = \pi u^2$ with initial value $u(x, 0) = \sin(2\pi x)$. So we can use exacly the same mesh as above with $a = 0, b = 1$. And since the initial value is a periodic function, we can also impose periodic BCs here.

In upwind and generalized MUSCL, we use the conservative FDM:
$u_j^{n+1} = u_j^n - \lambda\left(\hat{f}\left(u_j^n, u_{j+1}^n\right) - \hat{f}\left(u_{j-1}^n, u_j^n\right)\right)$ with previously proposed numerical flux. In LW and BW we use the generalization in the textbook: use Taylor expansion $u_j^{m+1} = [u + \tau u_t + \frac{1}{2}\tau^2 u_{tt}]_j^m + O(\tau^3)$ and choose appropriate methods to approximate $u_t = -(f(u))_x$ and $u_{tt} = [f'(u)(f(u))_x]_x$. In the case of LF we just use the central differencing scheme $\frac{f(U_{j+1}^m) - f(U_{j-1}^m)}{2h}, \frac{f(U_{j+1}^{m+1}) - f(U_{j-1}^{m+1})}{2h}$ to approximate $(f(u))_x$ at the node (j, m). In CN method since we are unable to solve nonlinear equations we would expect that we can derive linear equations as above. So we try to treat the PDE as $u_t + 2\pi u u_x = 0$ and we can use $2\pi u_j^m$ to approximate the velocity $2\pi u$ at the node (j, m). Then we can regard it as an Advection equation with variable a at each node. Approximate this equation in the same way as the CN method does above we can give a generalization of CN method.
More precisely, the 6 methods in this case can be listed as below:
The explicit upwind scheme (with $\hat{f}$ the upwind numerical flux):

$$\frac{u_j^{n+1} - u_j^n}{\tau} + \frac{\hat{f}(u_j^n, u_j^{n+1}) - \hat{f}(u_{j-1}^n, u_j^n)}{h} = 0$$

The LF scheme:

$$\frac{u_j^{n+1} - \left(u_{j+1}^n + u_{j-1}^n\right)/2}{\tau} + \frac{f(u_{j+1}^n) - f(u_{j-1}^n)}{2h} = 0$$

The LW scheme (with $a_{j+1/2}^n$ defined as above):

$$\frac{u_j^{n+1} - u_j^n}{\tau} + \frac{f(u_{j+1}^n) - f(u_{j-1}^n)}{2h} - \frac{\tau}{2h^2}\left[a_{j+\frac{1}{2}}^n(f(u_{j+1}^n) - f(u_j^n)) - a_{j-\frac{1}{2}}^n(f(u_j^n) - f(u_{j-1}^n))\right] = 0$$

The BW scheme:

$$\frac{u_j^{n+1}-u_j^n}{\tau}+\frac{3f(u_j^n)-4f(u_{j-1}^n)+f(u_{j-2}^n)}{2h}-\frac{\tau}{2h^2}\left[a_{j-\frac{1}{2}}^n(f(u_j^n)-f(u_{j-1}^n))-a_{j-\frac{3}{2}}^n(f(u_{j-1}^n)-f(u_{j-2}^n))\right]=$$

The CN scheme:

$$\frac{u_j^{n+1}-u_j^n}{\tau}+\pi u_j^m\frac{u_{j+1}^n-u_{j-1}^n}{2h}+\pi u_j^m\frac{u_{j+1}^{n+1}-u_{j-1}^{n+1}}{2h}=0$$

The generalized MUSCL scheme:

$$u_j^{n+1}=u_j^n-\lambda\left(\hat{f}(u_j^n+\frac{h}{2}S_j^n,u_{j+1}^n-\frac{h}{2}S_{j+1}^n)\ -\hat{f}(u_{j-1}^n+\frac{h}{2}S_{j-1}^n,u_j^n-\frac{h}{2}S_j^n)\right),$$

where all the notation here follows the definition as above.

3 Error estimation

We next shall briefly discuss the error estimaion in the 4th problem. We use $||\cdot||_2$ and $||\cdot||_\infty$ here, to be precise (assume we have $x_0<x_1<\cdots<x_N$):

$$||u||_2\approx\left(\sum_{j=0}^N u(x_j)^2\times\frac{1}{N}\right)^{\frac{1}{2}},||u||_\infty\approx\max_{0\le j\le N}|u(x_j)|.$$

But since we don't have the real solution at hand, we can only use posterior estimation of error. Here we try to consider $E(h)=||U_h-U_{h/2}||=||e_h-e_{h/2}||$, where the error $e=U-u$, u is the real solution and U is the numerical solution. If we assume the error is of α order we can write $U_{h,j}=u_j+C_jh^\alpha+o(h^\alpha)$, then we have $U_{h,j}-U_{h/2,j}=(1-2^{-\alpha})C_jh^\alpha+o(h^\alpha)$ when h is small enough. Moreover we have the approximation:

$$\ln||U_h-U_{h/2}||\approx\ln((1-2^{-\alpha})C)-\alpha\ln h^{-1}.$$

So we can set down $E(h)$ for different h and draw the above loglog plot. Then use a line to fit the obtained data we can get the convergence rate α as well as the constant C. Use the approximation $||e_h||\approx Ch^\alpha$ we can get a reasonable estimation of the error.

In real application we shall test the result for $N=4,8,\cdots,1024$ and calculate $E(h)$ for each two adjacent cases. Negelect all the case when the error does not decrease (we think the increase of error with finer grid may be caused by the failure of the above derivation) and we use linear function to fit data and make further inference.
As for the temporal step size, since the grid ratio τ/h is essential as shown by our later numerical results. We shall here choose an appropriate step size to avoid explosion that may occurred in this problem. So the grid ratio is not fixed, but we shall all reach the same time $t=0.015$ and use the above two norm to estimate the error $E(h)$.

4 Numerical results

Finally we shall give the numerical results. In the first three problem we just show the function plot at different time point as the problem suggested. In the last problem there's a jump point in the solutin after some time point. We shall give the error estimate and the convergence order before the jump point appeared and draw both the function plot before and after the jump point appeared.

4.1 Example 2.1

We give the function value at time $t = 0.5$ here. With grid ratio $\tau/h = 0.5$ fixed and $h = 0.01$ and $h = 0.0025$ for the computation domain $[0, 1]$. Some discussions:

- The results show these methods' different behaviours in coping with the discontinuity and the resolution can all be improved as the mesh is refined, namely the solution is more close to the real one with finer mesh.
- The first order method, upwind and LF, perform the worst in this case. They cannot simulate the discontinuity and only derive a smooth approximation.
- LW, BW, CN can simulate the jump better. But BW will generate oscillation after the jump whereas LW and CN will generate oscillation before the jump and the oscillation in CN is in effect for longer distance. LW and BW only generates short-distance oscillation. Moreover, MUSCL gives the best result in this case, producing an almost perfect simulation.

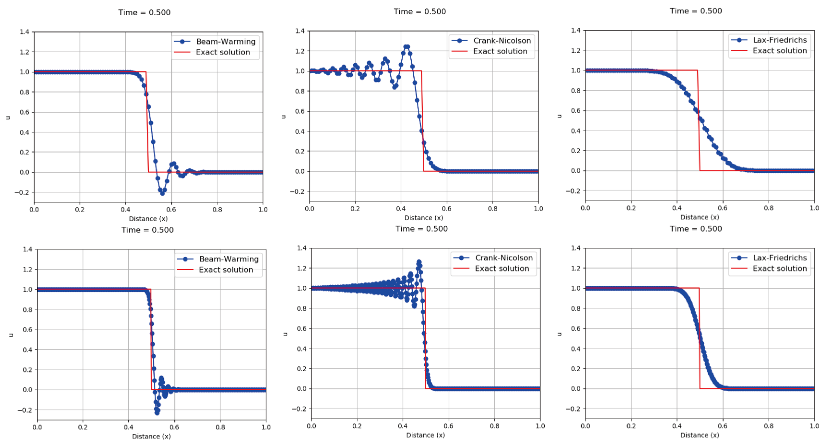

Figure 1: The numerical solution for the example 2.1 for the Beam-Warming (BW), Crank-Nicolson (CN) and Lax-Friedrichs (LF) methods at time $t = 0.5$. The first line is for $h = 0.01$ and the second line for $h = 0.0025$.

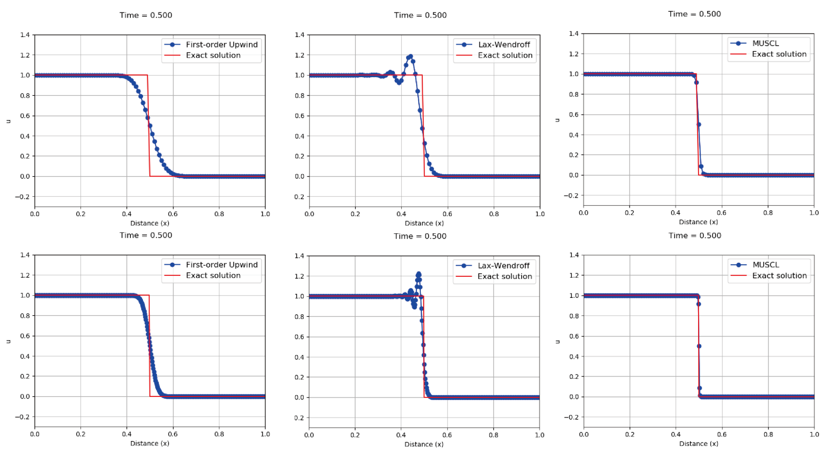

Figure 2: The numerical solution for the example 2.1 for the upwind, Lax-Wendroff (LW) and the generalized MUSCL methods at time $t = 0.5$. The first line is for $h = 0.01$ and the second line for $h = 0.0025$.

4.2 Propagation of a wave packet:

We give the function value at time $t = 2, 4, 8$ here, with $h = 1/200, \tau = 0.8h$, and $k = 80$ for the computation domain $[0, 1]$. Some discussions:

- The choice of grid ratio τ/h is essential. Though we use $\tau/h = 0.8$ for the other methods, in the case of MUSCL this ratio can produce explosion and unstability. So we use $\tau/h = 0.6$ in MUSCL and 0.8 in all the other cases.

- The first order methods, LF and upwind, produce the worst results. Whereas upwind can generate little oscillation at $t = 2$, LF is just flat at that time. So compared with upwind, LF may be worse in this case.

- MUSCL also produce almost perfect simulation in this case.

- As time moves on, we can see the real solution will move forward as the dynamic plot can display. Our numerical solution has also such a property. But as time moves on our numerical solution may also disperse: the magnitude of the signal is decreaing as time goes from 2 to 8 (except for MUSCL, upwind and LF).

- BW's signal will move before the real signal whereas LW's signal will leave behind. Compared with BW and LW, CN will also leave behind, but with a slower speed than LW. And as time went on, its influence domain is becoming much larger than the other two.

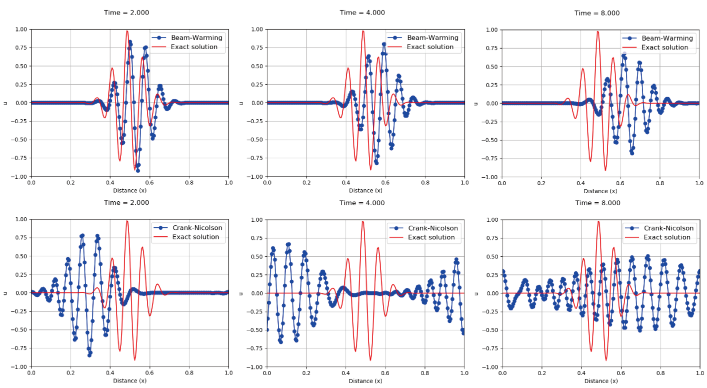

Figure 3: The numerical solution at time $t = 2, 4, 8$ for the BW (above) and CN (below) methods. One row is for one method.

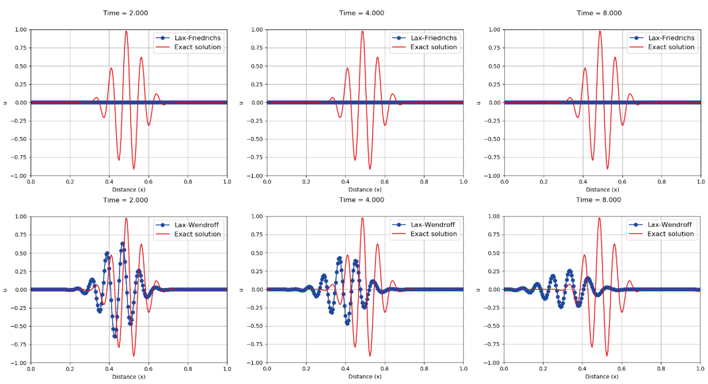

Figure 4: The numerical solution at time $t = 2, 4, 8$ for the LF (above) and LW (below) methods. One row is for one method.

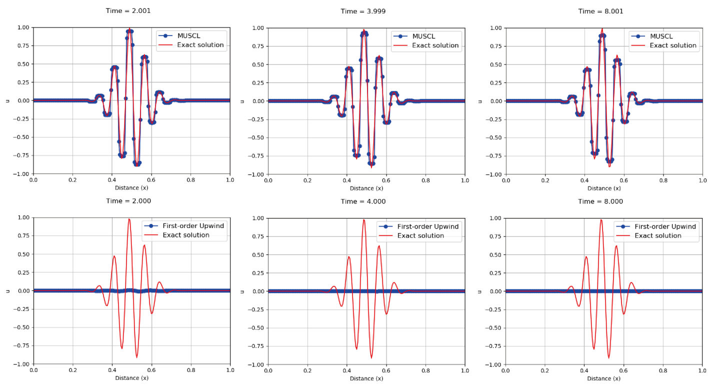

Figure 5: The numerical solution at time $t = 2, 4, 8$ for the generalized MUSCL (above) and upwind (below) methods. One row is for one method.

4.3 Highly discontinous data:

We give the function value at time $t = 8$ here, with $h = 1/500, \tau = 0.8h$ for the computation domain $[-1, 1]$. Some discussions:

- MUSCL performs ordinary here. Though it can simulate the jump behavior perfectly, it cannot simulate the smooth change well.
- The first methods, upwind and LF, give bad performance. Though they can simulate the smooth change well, it cannot simulate the jump behavior. They can also simulate a rough trend in this case.
- LW and BW gives the best results in this case and LW performs better. LW may produce oscillations behind of the discontinuity and BW will produce oscillations before it.
- CN can also simulate the solution well, but with greater oscillations compared with BW and LW. And the oscillations continue for the whole process,m unlike LW and BW, whose oscillations are local.

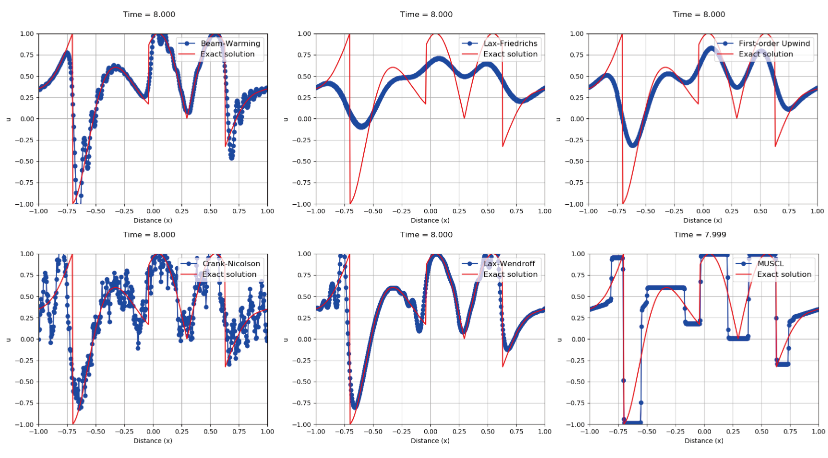

Figure 6: The numerical solution at time $t = 8$ for the highly discontinuous initial data obatined by using the 6 methods: BW, LF, Upwind, CN, LW, MUSCL (from left to right, from up to down).

4.4 Burgers equation:

We give the function value at time $t = 0.015$ (before the discontinuity appear) and $t = 0.05$ (after the discontinuity appear), with $\tau = 0.001$ and $h = 1/200$. Some discussions:

- At the time $t = 0.015$, all the methods generating almost the same function values.
- At time $t = 0.05$ we can see except for CN and BW, all the methods generate almost the same plot. And CN and BW may generate explosion (the function value is tend to infinity and produces NAN). This behavior is more severe for CN.
- As for the convergence order we can see except for MUSCL and upwind, all the methods can have approximately second order accuracy rate. MUSCL and upwind can have approximately first order accuracy rate.
- As for the error, CN has the smallest error. Then LW, BW and MUSCL almost perform at the same level. The upwind and LF perform the worst. Note though MUSCL is of first order, its performance can be compared with those second order methods. And even if LF is of second order in this case, its performance does not improve much compared with upwind.
- The choice of the mesh ratio is essential for some methods. When the ratio is too big some methods may generate explosion and lead to instability. So we will tune the ratio in this problem. When calculating the convergence order we shall usually fix the time step size, but sometimes we may adjust it.

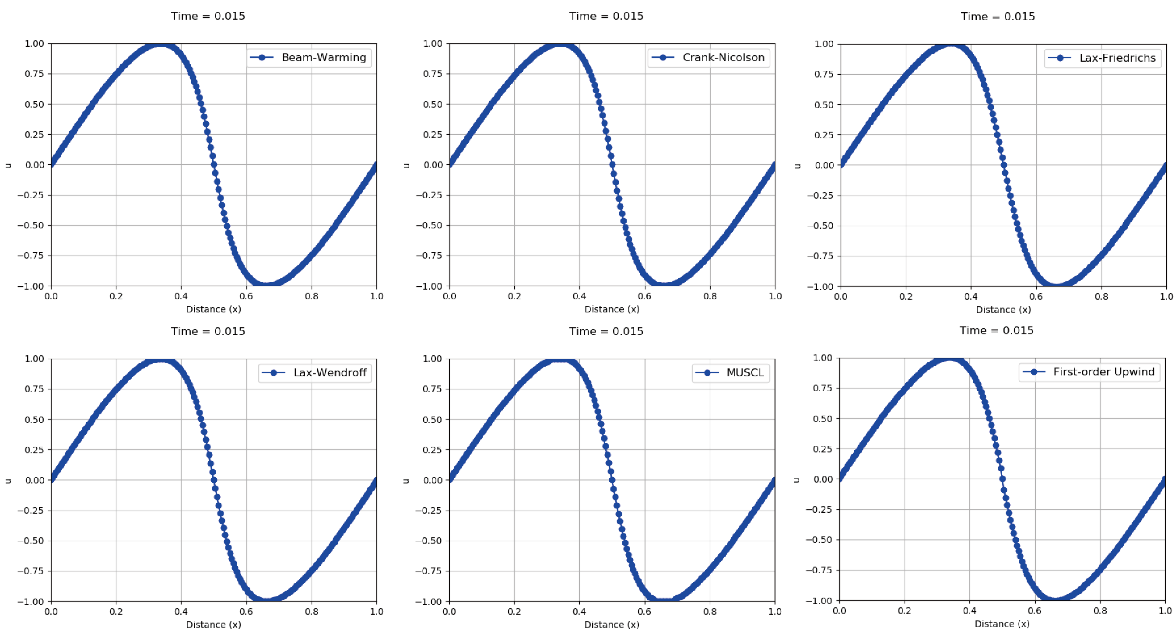

Figure 7: The numerical solution at time $t = 0.015$ before the discontinuity appear for the Burgers equation obatined by using the 6 methods: BW, LF, Upwind, CN, LW, MUSCL (from left to right, from up to down).

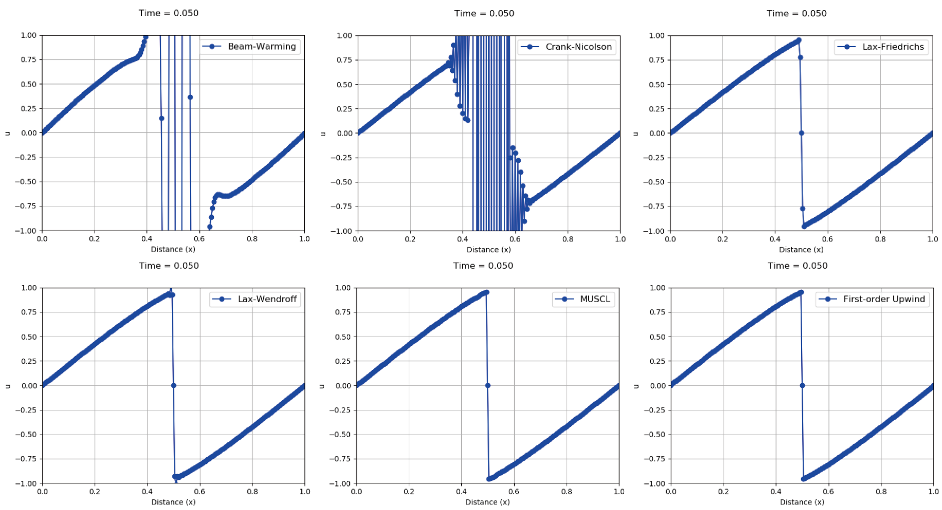

Figure 8: The numerical solution at time $t = 0.05$ after the discontinuity appear for the Burgers equation obatined by using the 6 methods: BW, LF, Upwind, CN, LW, MUSCL (from left to right, from up to down).

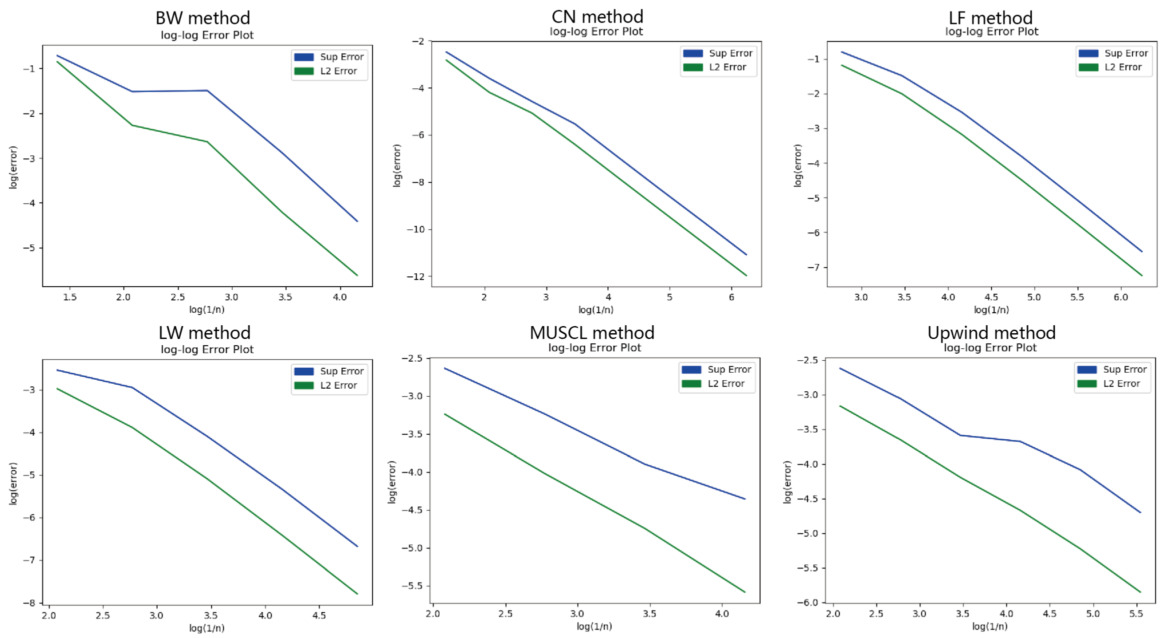

Figure 9: The convergence curve for the 6 methods.

Methods	CN	LF	LW	BW	MUSCL	Upwind
L_2 error	2.17e-4	0.02171	1.027e-3	0.003115	4.319e-3	0.01523
L_2 order	1.8848	1.7804	1.7544	1.6562	1.1183	0.7678
L_∞ error	5.03e-4	0.04096	3.508e-3	0.01866	0.01901	0.05337
L_∞ order	1.7758	1.6944	1.5393	1.2637	0.839	0.5591

Table 1: The error and convergence rate (order) for the 6 methods in the $||\cdot||_2$ and $||\cdot||_\infty$ norms. The order is calcualted by fitting a linear function to the data. The error is calcualted through the fitted linear functions, i.e. we use Ch^α to compute the error with C, α computed through line fitting and we set $h = 1/100$.